Title:

# Population structure of the scleractinian coral, Montastraea cavernosa, in southeast Florida

Authors:

Dodge DL, Studivan MS, Eckert RJ, Chei E, Beal J, Voss JD

DOI:

https://doi.org/10.5343/bms.2019.0074

Date submitted: 24 July, 2019

Date accepted: 16 December, 2019

Available online: 17 December, 2019

Citation:

Dodge DL, Studivan MS, Eckert RJ, Chei E, Beal J, Voss JD. In Press. Population structure of the scleractinian coral, Montastraea cavernosa, in southeast Florida. Bulletin of Marine Science. https://doi.org/10.5343/bms.2019.0074

# Population structure of the scleractinian coral, *Montastraea cavernosa*, in Southeast Florida

Running Title: Southeast Florida *M. cavernosa* population structure

Dodge, D. L.[1]
Studivan, M. S.[1]
Eckert, R. J.[1]
Chei, E.[1]
Beal, J.[2]
Voss, J. D.[1]

Author Affiliations
[1]Harbor Branch Oceanographic Institute, Florida Atlantic University, Fort Pierce, Florida 34946
[2]Florida Fish and Wildlife Conservation Commission, Fort Pierce, Florida 34974
*Correspondence: Joshua Voss; jvoss2@fau.edu

ABSTRACT

The persistence of scleractinian coral populations on the Florida Reef Tract (FRT) is controlled in part by metapopulation dynamics and larval dispersal. Nine polymorphic microsatellite loci were analyzed to identify contemporary population structure and gene flow as well as historical migration rates of *Montastraea cavernosa* at five sites off Martin, Palm Beach, and Broward Counties in Southeast Florida. The sampled populations demonstrated evidence of genetic isolation by distance over a geographic range of 85 km. Population genetic structure was divided into two genetic clusters, northern and southern, with admixture along a latitudinal gradient. Historical migration models indicated likely panmixia throughout all sites sampled, identifying a potential reduction in connectivity among the sampled populations through time. Though *M. cavernosa* populations demonstrated evidence of historical connectivity, contemporary patterns of isolation by distance suggest that effective management will require localized actions to maximize the likelihood of sustaining individual populations in the northern FRT. Given the results of this study, coupled with recent coral mortality events in the region, we recommend regional conservation efforts and management initiatives throughout Southeast Florida within a more comprehensive FRT-wide management network.

## INTRODUCTION

Coral reefs ecosystems, and their valuable coastal ecosystem services, have experienced dramatic declines globally since the 1980s (Gardner et al. 2003, Bruno and Selig 2007, Edmunds 2015). Nearshore coral reefs in the Florida Reef Tract (FRT) have suffered severe losses in the past several decades due to increased stressors including land-based sources of pollution, sedimentation, diseases, and thermal stress (Lirman and Fong 2007, Lirman et al. 2011, Ruzicka et al. 2013, Manzello 2015, Precht et al. 2016, Walton et al. 2018). As the third largest barrier reef system in the world, the FRT extends 595 km between the Dry Tortugas in the southwest and Martin County to the north. Towards the northern limit, this reef system reaches a marginal ecotone between subtropical and warm temperate climate zones (Lugo et al. 1999) with increased environmental variability but diverse marine communities (Beal et al. 2012). The northern FRT (NFRT) in Martin County represents the latitudinal limit in the continental United States for most tropical scleractinian species (Reed 1985). Despite lower coral cover and coral species diversity as compared to relatively well-studied reef systems in the Florida Keys and wider Tropical Western Atlantic, this marginal environment is a significant resource to the local economy and coastal ecosystems (Johns et al. 2004, Collier et al. 2008, Gilliam et al. 2015). Though long-term monitoring and mapping efforts are ongoing (Banks et al. 2007, Walker and Gilliam 2013, Walton et al. 2018), levels of connectivity and gene flow among coral populations in the NFRT are largely unknown.

Understanding patterns of population structure and reef connectivity have become critical in the design and implementation of effective management and restoration strategies. In benthic species, population structure is often driven by larval dispersal (Cowen and Sponaugle 2009), allowing exchange of gametes among populations and possibly an increase in genetic variation

required for evolutionary adaptation (van Oppen and Gates 2006). For corals, dispersal potential is dependent on larval characteristics, including spawning strategy (broadcast spawning versus brooding), pelagic larval duration, settlement/survival rates (Cowen and Sponaugle 2009), as well as oceanographic patterns conducive to larval transport. Along the East coast of Florida, the northward-flowing Florida Current, seasonal upwelling, and counter-current eddies are notable influences that can impact distribution of coral larvae (Limouzy-Paris et al. 1997, Hare and Walsh 2007). Hydrological features and larval characteristics can vary substantially across habitats and coral species, resulting in highly divergent patterns of population connectivity at local and regional scales (Nunes et al. 2011, Bongaerts et al. 2017, Studivan and Voss 2018a, Eckert et al. 2019).

Habitat ranges, larval characteristics, and dispersal potential are difficult to quantify for most marine species including corals (Palumbi 2003, Cowen and Sponaugle 2009). Fortunately, population connectivity across broad temporal and spatial scales can also be investigated through analyses of genomic variations. Population genetic approaches have been commonly used in marine conservation applications, particularly for coral reef ecosystems (Palumbi 2003, Gutiérrez-Rodríguez and Lasker 2004, van Oppen and Gates 2006, Beger et al. 2014, Aswani et al. 2015, Studivan and Voss 2018b). For example, population genetic tools are frequently used in the implementation and design of Marine Protected Areas (MPAs), design of sustainable fisheries, and marine spatial planning through the identification of important metapopulations (Ward et al. 2001, Palumbi 2004). Microsatellite markers, or simple sequence repeats (SSRs), are one common, cost-effective method for investigating population genetic patterns among scleractinian species and geographic locations to answer such conservation-related questions

(Miller and Howard 2004, Shearer and Coffroth 2004, Vermeij et al. 2006, Beger et al. 2014, Porto-Hannes et al. 2015).

Previous studies examining population structure across several coral species in the Florida Keys and southern FRT have suggested relatively high connectivity among populations (Baums et al. 2010, Hemond and Vollmer 2010, Serrano et al. 2014, 2016, Manzello et al. 2019). A recent study suggested the potential for divergence between populations of *Acropora cervicornis* in the Florida Keys and those in Broward County (Drury et al. 2017), identifying a potential break between northern and southern regions of the FRT. Limited data exists for coral reefs in the NFRT, representing a critical data gap. In conjunction with knowledge of oceanographic patterns influencing larval dispersal, genetic data can inform management strategies that enhance the likelihood of regional survivorship and aid in successful recruitment among downstream populations. Efforts to protect corals reefs along the FRT from further degradation have led to the creation of a Southeast Florida Coral Reef Ecosystem Conservation Area (ECA; FL 2018 House Bill 53; Fig. 1) which extends from St. Lucie Inlet to Biscayne National Park. This study was designed to address the population connectivity data gaps in the NFRT and to inform management strategies for the newly established ecosystem conservation area.

*Montastraea cavernosa* is one of the dominant scleractinian coral species in the NFRT and is commonly found throughout the wider Tropical Western Atlantic as a structurally important reef builder (Nunes et al. 2009). Larval characteristics for *M. cavernosa*, including its relatively large egg size and gonochoric broadcast spawning strategy, may enhance the distance traveled by larvae via oceanographic currents (Szmant 1991). The pelagic larval duration and competency period have not been quantified for this species, but are suspected to be relatively

long due to observed levels of gene flow among geographically disparate populations. Previous population genetics studies identified broad connectivity across geographic regions in excess of 1,000 km (Nunes et al. 2009, Goodbody-Gringley et al. 2012) and vertically among depths in some regions (Brazeau et al. 2013, Serrano et al. 2014, Studivan and Voss 2018a, Eckert et al. 2019). As a common and ecologically important coral in the NFRT, *M. cavernosa* represents an ideal species to examine population structure at multiple spatial scales, allowing inferences to be made across regions and within coral reef habitats of critical ecological and economic importance, such as those found in Florida.

## METHODS

### *Coral sampling*

Five sites were chosen to assess latitudinal connectivity of *M. cavernosa* along the NFRT: St. Lucie Reef (SLR) in Martin County, Jupiter (JUP), West Palm Beach (WPB), and Boynton Beach (BYN) in Palm Beach County, and Fort Lauderdale (FTL) in Broward County (Fig. 1). At all locations, coral colonies were selected based on colony size (~20–100 cm diameter), apparent health (no signs of bleaching or disease), and >1 m distance from other sampled colonies to reduce the likelihood of clonal samples. Fragments of coral tissue and skeleton approximately 5 $cm^2$ in size were collected from the margin of colonies using a hammer and chisel and placed in individual zip-top bags filled with ambient seawater (Table 1). Fragments were transferred to individual tubes and preserved in TRIzol (St. Lucie Reef, Jupiter, West Palm Beach) or molecular grade ethanol (Boynton Beach, Fort Lauderdale) and stored at -80 °C until further processing. Differences in sample preservation were due to changes in

protocol to reduce user hazards and increase temperature stability of preserved samples; both preservatives yielded sufficient quality genomic DNA for downstream analyses.

*DNA extraction and genotyping*

Frozen TRIzol samples were thawed at room temperature (~1–2 h) and processed with a modified phenol-chloroform DNA extraction (Chomczynski and Sacchi 2006; https://github.com/mstudiva/Mcav-microsats). Genomic DNA from ethanol-preserved samples was extracted using a modified Cetyl trimethylammonium bromide (CTAB) extraction protocol (Mieog et al. 2009) as described in Eckert et al. (2019). The resulting DNA pellets were eluted in Tris EDTA (TE) pH 8.0 and incubated at 55 °C for 10 minutes. DNA extracts were cleaned with the Zymo DNA Clean & Concentrator-5 Kit to remove extraneous proteins and PCR inhibitors. The concentration and quality of all cleaned DNA samples were measured with a NanoDrop 2000 (Thermo Fisher Scientific), and DNA was diluted to a concentration of 10 ng $\mu L^{-1}$.

Nine previously-developed microsatellite loci (Serrano et al. 2014) were amplified in all samples with a multiplex PCR using the Qiagen Type-It Microsatellite PCR kit, universal forward primers fluorescently-labeled with NED, VIC, or 6-FAM, and reverse primers (Blacket et al. 2012; Table S1). PCR thermal cycling consisted of the following: 95 °C for 5 min (initial denaturation), 30 (ethanol samples) or 35 (TRIzol samples) cycles of 30 sec at 95 °C (denaturation), 60 °C for 90 sec (annealing), 72 °C for 30 sec (extension), and 60 °C for 30 min (final extension). Additional PCR cycles were necessary for TRIzol samples due to variable initial DNA quality.

Amplified alleles were visualized on a 2% agarose gel to verify amplification success and to select dilution strength based on band intensity. PCR products were diluted and sized with an Applied Biosystems 3130 XL (500 ROX size standard) at Florida Atlantic University's Harbor

Branch Oceanographic Institute. Resulting electropherograms were analyzed and alleles were scored with GeneMapper v3.7 (Applied Biosystems). Samples with low or unidentifiable allele peaks at individual loci were re-amplified to correct for incomplete data. Samples were run a mean of 1.3 times per locus on the genetic analyzer to ensure sufficient coverage across all loci. After re-amplification attempts, samples missing data at more than three loci were removed from further analyses.

*Genetic and statistical analyses*

Multilocus genotypes (MLGs) and violations of Hardy-Weinberg Equilibrium (HWE) across loci were identified in GenAlEx v6.5 (Peakall and Smouse 2012). Genetic diversity metrics, including population differentiation, fixation index ($F_{ST}$), and Nei's genetic distance ($D_A$) were calculated in GenAlEx. Private alleles per locus within populations were determined using the *R* package *diveRsity* (Keenan et al. 2013). Linkage disequilibrium (LD) assumptions were tested in Arlequin v3.5 (Excoffier and Lischer 2010). All *p*-values for HWE, LD, and $F_{ST}$ were corrected for false discovery rate (FDR; Benjamini and Hochberg 1995). Violations of HWE and LD assumptions were tested for significant impact of null alleles, where null allele-corrected $F_{ST}$ values were calculated using FreeNA (Chapuis and Estoup 2007), then compared to raw $F_{ST}$ values using correlation analyses across populations and loci. Loci were examined for HWE and LD violations and patterns of allelic richness across populations, to determine if any loci needed to be removed prior to downstream analyses. An analysis of molecular variance (AMOVA) was calculated among individuals and populations using GenAlEx with 9,999 permutations. A principal coordinates analysis (PCoA) visualized genetic distance between populations using Nei's genetic distance, and a Mantel isolation by distance test assessed the

relationship between genetic and geographic distance in GenAlEx (9,999 permutations) using over-water distances calculated from site GPS coordinates.

Structure v2.3.4 (Pritchard et al. 2000) was used to analyze genetic structure and identify populations. Samples were assigned to *K* populations in a probabilistic manner until HWE and linkage equilibrium was achieved, assuming that loci were unlinked and freely recombine. Using an admixture model, simulations were run with $10^6$ Markov Chain-Monte Carlo (MCMC) replications after a 1,000 burn-in period. The number of postulated populations (*K*) was tested between 1–8 with 10 replicate tests per value of *K*. Structure output results were analyzed using the web-based Structure Harvester (Earl and VonHoldt 2012) to determine the most likely value of *K* using the Evanno method (Evanno et al. 2005). A combined structure plot of all replicate simulations for the highest likelihood *K* was created to represent individual membership to genetic clusters using CLUMPP v1.1.2 (Jakobsson and Rosenberg 2007) and Distruct v1.1 (Rosenberg 2004).

Historical migration rates of ancestral *M. cavernosa* populations (~$4N_e$ generations) among sites were estimated with Migrate-n v3.6.11 (Beerli 2006, Beerli and Palczewski 2010) using Bayesian inference to determine the maximum likelihood of various genetic migration models. Generation times and mutation rates for microsatellite loci are unknown for most coral species (but see Devlin-Durante et al. 2016). Because *M. cavernosa* is a relatively long-lived and reproductively viable at an early age (Szmant 1991, Soong 1993), the migration estimates provided by Migrate-n represent patterns over hundreds to thousands of years. Four possible migration models were tested: (1) symmetrical migration across all sites; (2) unidirectional migration from southern to northern sites; (3) unidirectional migration from northern to southern sites; and (4) panmixia. All models allowed stepwise migration, where upstream populations

193 could contribute migrants to all downstream populations (and vice versa for the symmetrical
194 migration model). All migration models were run with the following parameters: 20 replicates,
195 long-inc 100, long-sample 15,000, burn-in 20,000, and 4 heated chains (1, 1.5, 3, $10^5$). Prior
196 distributions for mutation-scaled population size ($\Theta$) and mutation-scaled immigration rate ($M$)
197 were set from 0–100 and 0–1,000, respectively. The most likely migration scenario was
198 determined by ranking of Bezier log marginal likelihoods (*ln(mL)*) for each model using the
199 thermodynamic integration method described in Beerli and Palczewski (2010). To assess
200 whether the genetic divergence of the Fort Lauderdale population from all other populations may
201 have been driving historical migration results, the model scenarios were repeated excluding Fort
202 Lauderdale from the dataset.

203

204 RESULTS

205 Of the nine microsatellite markers amplified in this study, eight consistently met HWE
206 assumptions across populations (Table S2). No violations of LD assumptions were observed
207 across loci or populations. In addition to HWE violations in three out of five sampled
208 populations, locus MC4 demonstrated abnormally high number of alleles ($N_a$) and allelic
209 richness ($A_r$; Table S2). Allele bins within locus MC4 were also close to one another,
210 compromising the ability to definitively make allele calls. MC4 was therefore removed from all
211 further analyses. Subsequent analyses using the remaining dataset identified no clonal MLGs
212 within the populations, allowing all amplified samples to be used for statistical assessments of
213 genetic connectivity. Null allele-corrected $F_{ST}$ values were found to be tightly correlated with
214 raw $F_{ST}$ values across loci and populations ($R^2 = 0.9926$ and $R^2 = 0.9976$, respectively); therefore
215 raw values were reported.

Allelic diversity was similar among populations, with an overall mean range of allelic richness ($A_r$) between 3.54–19.50. Fort Lauderdale demonstrated the lowest richness ($A_r$ = 2.79), while Jupiter had the greatest ($A_r$ = 22.75). Expected heterozygosity ($H_e$) was also similar among populations, with Fort Lauderdale once again having the lowest ($H_e$ = 0.16) and Jupiter having the highest ($H_e$ = 0.95). The global fixation index ($F_{ST}$) was 0.017 across all populations. An analysis of molecular variance (AMOVA) indicated that 6% of genetic variation was within populations (df = 149, SS = 436.932, $p$ = 0.0001), while only 2% of this variation was among populations (df = 4, SS = 23.888, $p$ = 0.0001). PCoA demonstrated clustering of northernmost sites St. Lucie Reef and Jupiter, indicating high genetic similarity of these populations (Fig. 2). Genetic distance among sites reflected site geography, with West Palm Beach and Boynton Beach being intermediately distinct, and the southernmost site Fort Lauderdale being the most distant population. Pairwise population $F_{ST}$ values reinforced the PCoA results, indicating that Fort Lauderdale was significantly differentiated from all other sites, and supporting genetic isolation of sites by distance (Fig. 3). The Mantel test revealed a significant correlation between geographic distance and Nei's genetic distance ($R^2$ = 0.3946, $p$ = 0.033; Fig. 4). Geographic distances among pairwise comparisons of sites ranged from 21.65 to 84.57 km.

A Bayesian population clustering model in Structure identified the most likely number of genetic clusters ($K$) among populations to be $K$ = 2 through both log model likelihood (L($K$)) and the Evanno method (Fig. 5; Table S3; Fig. S1). Northernmost sites St. Lucie Reef and Jupiter exhibited similar genetic structure and were derived predominantly from a single genetic cluster represented by dark blue in Fig. 5. The southernmost site Fort Lauderdale was dominated by a separate genetic cluster represented by light blue. Intermediate sites West Palm Beach and

Boynton Beach showed admixture from both populations; however, both were primarily represented by the same genetic cluster observed at the northern sites (dark blue).

Assessment of historical population migration using Migrate-n indicated panmixia among all sampled populations. Model likelihood for panmictic migration was much higher than for other tested models simulating stepwise symmetric, south-north, and north-south migration, with near-zero probabilities for the latter models (Table 2). Repeated model simulations using a dataset excluding Fort Lauderdale demonstrated that panmixia was once again the most likely migration scenario, with all other migration models showing near-zero probabilities. Estimated population sizes for both likely models are given in Table 2.

## DISCUSSION

This study provides evidence that populations of an important reef-building coral, *Montastraea cavernosa*, in the northern Florida Reef Tract were historically well-connected. However, examination of contemporary population structure and gene flow among *M. cavernosa* populations in the NFRT identified patterns of genetic differentiation. *Montastraea cavernosa* exhibits relatively high levels of horizontal gene flow across its range, and particularly throughout the Florida Keys, Gulf of Mexico, Belize, Barbados, Bermuda, Jamaica, and Panama (Nunes et al. 2009, Goodbody-Gringley et al. 2012, Serrano et al. 2014, Studivan and Voss 2018a, Eckert et al. 2019). Certain larval characteristics are thought to increase the ability of pelagic larvae to survive and therefore travel long distances, thus increasing population connectivity throughout a larger region (Hare and Walsh 2007). The relatively large egg size of *M. cavernosa*, broadcast spawning reproductive mode, and pelagic larval duration period may enable broad transport of larvae across geographically-isolated areas (Szmant 1991, Acosta and

261 Zea 1997, Jones et al. 2009), provided oceanographic patterns allow transport among reefs.
262 While pelagic larval duration and competency periods have not been quantified for *M.*
263 *cavernosa*, it is not suspected that larval characteristics reduce this species' dispersal potential,
264 given the evidence of connectivity observed over ranges exceeding 1,000 km (Nunes et al. 2009,
265 2011, Goodbody-Gringley et al. 2012, Studivan and Voss 2018a).

266 Oceanographic patterns are likely the main driver of larval transport and gene flow
267 among populations in Florida. The predominant Florida Current, which is fed by the consistently
268 strong (typically >1 m $s^{-1}$) Gulf of Mexico Loop Current through the Straits of Florida (Oey et al.
269 2005), runs nearly the entire length of the FRT and has the potential to transport larvae from the
270 southern to the northern extent of the FRT (Limouzy-Paris et al. 1997, Hare and Walsh 2007,
271 Sponaugle and Cowen 2019). Nearshore habitats also experience localized upwelling and
272 counter-current eddies that deviate shoreward from the Florida Current, which have been shown
273 to influence larval dispersal patterns (Limouzy-Paris et al. 1997, Sponaugle et al. 2005). Given
274 that hydrological features in the region have been predicted to be relatively consistent and
275 supportive of reef growth through the Holocene beginning ~12,000 ya (Banks et al. 2008), it is
276 not surprising that we observed historical panmixia in *M. cavernosa* populations across a linear
277 distance of ~85 km.

278 While *M. cavernosa* populations in the NFRT demonstrate historical connectivity based
279 on the Migrate-n results, there is additional evidence of relatively recent population
280 differentiation based on contemporary population structure and gene flow. Multiple analyses
281 demonstrate isolation by distance for *M. cavernosa* in the study region (Fig. 4). Additionally,
282 evaluation of population structure identified two dominant genetic clusters across the range of
283 sampled sites (Fig. 5). Northernmost sites St. Lucie Reef and Jupiter were nearly

indistinguishable from one another while the southernmost site, Fort Lauderdale, was also distinct. Admixture at intermediate sites West Palm Beach and Boynton Beach indicated variable influences of both genetic clusters across a latitudinal gradient. It is important to note, however, that observed differences in population structure among sites appeared to be largely driven by pairwise differences between Fort Lauderdale and all other sampled sites (Fig. 3). Given these observations, it appears that the dark blue genetic cluster common across the NFRT demonstrates higher genetic diversity than the light blue cluster predominantly found in Fort Lauderdale. For example, Jupiter was shown to have the highest allelic richness (also the highest membership to the dark blue cluster), while Fort Lauderdale had the lowest.

The results of these complementary analyses suggest that population sources are different between sites in Martin and Palm Beach Counties (St. Lucie Reef, Jupiter, West Palm Beach, and Boynton Beach) and those in Broward County (Fort Lauderdale). To our knowledge, no studies have examined coral population structure across all ranges of the FRT, but previous population genetics analyses of *A. cervicornis*, a broadcast spawning species, suggest a further divergence between populations in the Florida Keys and those in Broward County (Drury et al. 2017). It is therefore possible that coral populations may be split into zones along the FRT, with variable patterns of gene flow and genetic diversity within and among regions. The observed trends in this study may be further explained by variation in oceanographic patterns that occur at the northern extent of the FRT. Following the Atlantic continental shelf, the Florida Current diverges from the Florida coastline at the Bahamas Fault Zone where coastal morphology changes (Walker 2012). The two northernmost sites sampled for this study, St. Lucie Reef and Jupiter, are located north of the Bahamas Fault Zone, potentially reducing northward transport of larvae from southern populations. Subregional oceanographic features including eddies between

the Florida Current and nearshore habitats may be sufficient to allow gene flow over time, albeit at a lower rate of success with increasing latitude. This is perhaps best evidenced by the decreasing level of admixture between genetic clusters from southern to northern sites (Fig. 5).

The more recent population divergence observed in the NFRT may be indicative of habitat degradation and declines in *M. cavernosa* abundance along the FRT (Beal et al. 2012, Walton et al. 2018) with associated reductions in coral reproduction and recruitment. Coral cover and reef diversity have declined in recent decades in part due to macroalgal phase shifts (Palandro et al. 2008, Burman et al. 2012, Ruzicka et al. 2013), severe mortality events following thermal stress (Lirman et al. 2011), and disease outbreaks (Precht et al. 2016). Likewise, reduced coral recruitment has been observed elsewhere in the Tropical Western Atlantic (Hughes 1994, Mumby et al. 2007, Mumby 2009). Coral mortality events may constitute genetic bottlenecks, where winnowed coral populations can lead to decreased genetic diversity and gene flow. Spawning and recruitment have not been examined for most of the NFRT (but see Miller et al. 2000, Lirman and Fong 2007). Colony fate-tracking of *M. cavernosa* at St. Lucie Reef revealed no observed spawning in the past decade and no histological evidence of gamete production (Beal et al. 2012, Klepac et al. 2015). It may also be possible that exogenous *M. cavernosa* recruits still reach the NFRT but do not survive into adulthood or become reproductive members of the population.

*Implications for management*

Our results suggest that contemporary *M. cavernosa* populations in the NFRT do not appear to be a substantial contributor to regional larval supply. Instead, it is more likely that populations are considered sinks, with additional divergence between the northern (St. Lucie Reef, Jupiter, West Palm Beach, and Boynton Beach) and southern (Fort Lauderdale) regions of

the NFRT. There is a need to quantitatively track recruitment among populations on the FRT, allowing the identification of important source populations and perhaps the prioritization of regions in need of conservation initiatives, especially with respect to ongoing coral nursery and gene banking programs. Therefore, this study's results provide support for regional conservation through a network of small-scale management initiatives throughout Southeast Florida within a FRT-wide comprehensive network. Resolving patterns of genetic structure over small spatial scales is required to make informed local management guidelines, especially with diverse reef habitats in the NFRT where coral density is low and reproduction (both sexual and asexual) are reduced. Such factors decrease the ability and likelihood of these reefs to recover from mortality events, leading to an increased need to sustain and protect present resources. Informed management of coral reefs in the proposed Southeast Florida Coral Reef Ecosystem Conservation Area will require 1) additional sampling to fill in the gaps for the dominant coral, *M. cavernosa,* in southern Broward and Miami-Dade counties, and 2) similar approaches for additional targeted coral and fish species.

An increasing number of studies are examining multiple aspects of connectivity within regions, particularly in the comparison of genetic and biophysical connectivity (Galindo et al. 2006, Davies et al. 2017, Garavelli et al. 2018, Studivan and Voss 2018b). The FRT, with its dynamic current patterns and variable reef diversity across latitudes, would benefit greatly from studies of this nature. There is a critical need for detailed sampling and observation of distinct gradients in the region, ideally with molecular markers capable of higher resolution, such as single nucleotide polymorphism (SNP) loci (Drury et al. 2017, Manzello et al. 2019). This need is particularly acute given continued coral population declines resulting from the recent stony coral tissue loss disease outbreak along the FRT (Precht 2016, Walton et al. 2018).

## Author Contributions

JDV and JB designed and funded this research. DD, MS, JB, and JDV conducted coral sampling. DD, MS, RE, and EC performed microsatellite genotyping and statistical analysis. RE, MS, and EC created the figures. All authors contributed to the development and final editing of the manuscript.

## Funding and Permits

This project was supported by Florida Sea Grant R/LR-B-70 to JDV and JB, NOAA Coral Reef Conservation Program grant NA16NOS4820052 to JDV, EPA grant X700D66717 to JDV and JB, PADI Foundation grant 21853 to DD, a Women Divers Hall of Fame scholarship to DD, an Indian River Lagoon Graduate Research Fellowship to DD, and a donation from the River Branch Foundation. Corals were collected under Florida Fish and Wildlife Conservation Commission authority and Florida State Park Service permit 09231515.

## Acknowledgments

We are grateful to the St. Lucie Inlet Preserve State Park, Martin County, Florida Fish and Wildlife Conservation Commission, and the Florida Department of Environmental Protection Coral Reef Conservation Program for their collaboration and support of this research. We thank Alycia Shatters, Jennifer Polinski, Amanda Alker, Patrick Gardner, Alexis Sturm, Ian Combs, Cameron Luck, James Nelson, and Matthew Roy for outstanding diving and boat support. Tatiana Ferrer and Greg O'Corry-Crowe at FAU HBOI provided Applied Biosystems 3130 XL

375 sequencing services. This is contribution XXXX from FAU's Harbor Branch Oceanographic
376 Institute.

## Tables and Figures

Table 1: Site locations and genotyped samples for the northern Florida Reef Tract, with the number of collected samples ($n$) and multi-locus genotypes ($n_g$) used for the analyses. Geographic coordinates given as decimal degrees (WGS84).

| Population | Acronym | Site | Latitude | Longitude | $n$ | $n_g$ | Depth (m) | Collection Dates |
|---|---|---|---|---|---|---|---|---|
| St. Lucie Reef | SLR | | | | 34 | 31 | 5.0 | |
| | | SLR Central | 27.1317 | -80.1340 | 5 | 4 | 2.4 | Sep 2014–Oct 2015 |
| | | SLR Ledge | 27.1214 | -80.1275 | 24 | 22 | 9.7 | Jun 2013–Feb 2017 |
| | | SLR South | 27.1119 | -80.1255 | 5 | 5 | 3.0 | Dec 2012–Oct 2015 |
| Jupiter | JUP | | | | 31 | 30 | 21.0 | |
| | | Jupiter Ledge | 26.9440 | -80.0022 | 31 | 30 | 21.0 | Dec 2016 |
| West Palm Beach | WPB | | | | 35 | 30 | 17.7 | |
| | | Breaker's Reef | 26.7179 | -80.0187 | 35 | 30 | 17.7 | Jun 2015 |
| Boynton Beach | BYN | | | | 33 | 32 | 14.5 | |
| | | SEFL-16 | 26.5235 | -80.0316 | 33 | 32 | 14.5 | Jun 2018 |
| Ft. Lauderdale | FTL | | | | 31 | 31 | 13.6 | |
| | | BC1 | 26.1479 | -80.0960 | 9 | 9 | 8.2 | Jun 2018 |
| | | BC2 | 26.1600 | -80.0825 | 13 | 13 | 14.5 | Jun 2018 |
| | | BC3 | 26.1586 | -80.0774 | 9 | 9 | 18.2 | Jun 2018 |

Table 2. Comparison of Bezier log marginal likelihoods (*ln(mL)*) for migration models (symmetric migration, migration from south to north, migration from north to south, and panmixia) across all populations, and following the removal of Fort Lauderdale. Models were ranked according to likelihood values to calculate probabilities and rank. Mutation scaled population size ($\Theta$) included for the most probable model (± 95% CI).

| **Dataset** | **Model** | ***ln(mL)*** | **Probability** | **Rank** | **$\Theta$ (± 95% CI)** |
|---|---|---|---|---|---|
| All populations | symmetric | -871446 | 0 | 4 | |
| | south-north | -475069 | 0 | 3 | |
| | north-south | -288996 | 0 | 2 | |
| | panmixia | -26436 | 1 | 1 | 12.50 (4.87–10.27) |
| FTL removed | symmetric | -413402 | 0 | 4 | |
| | south-north | -78427 | 0 | 3 | |
| | north-south | -58799 | 0 | 2 | |
| | panmixia | -20073 | 1 | 1 | 8.49 (3.40–7.80) |

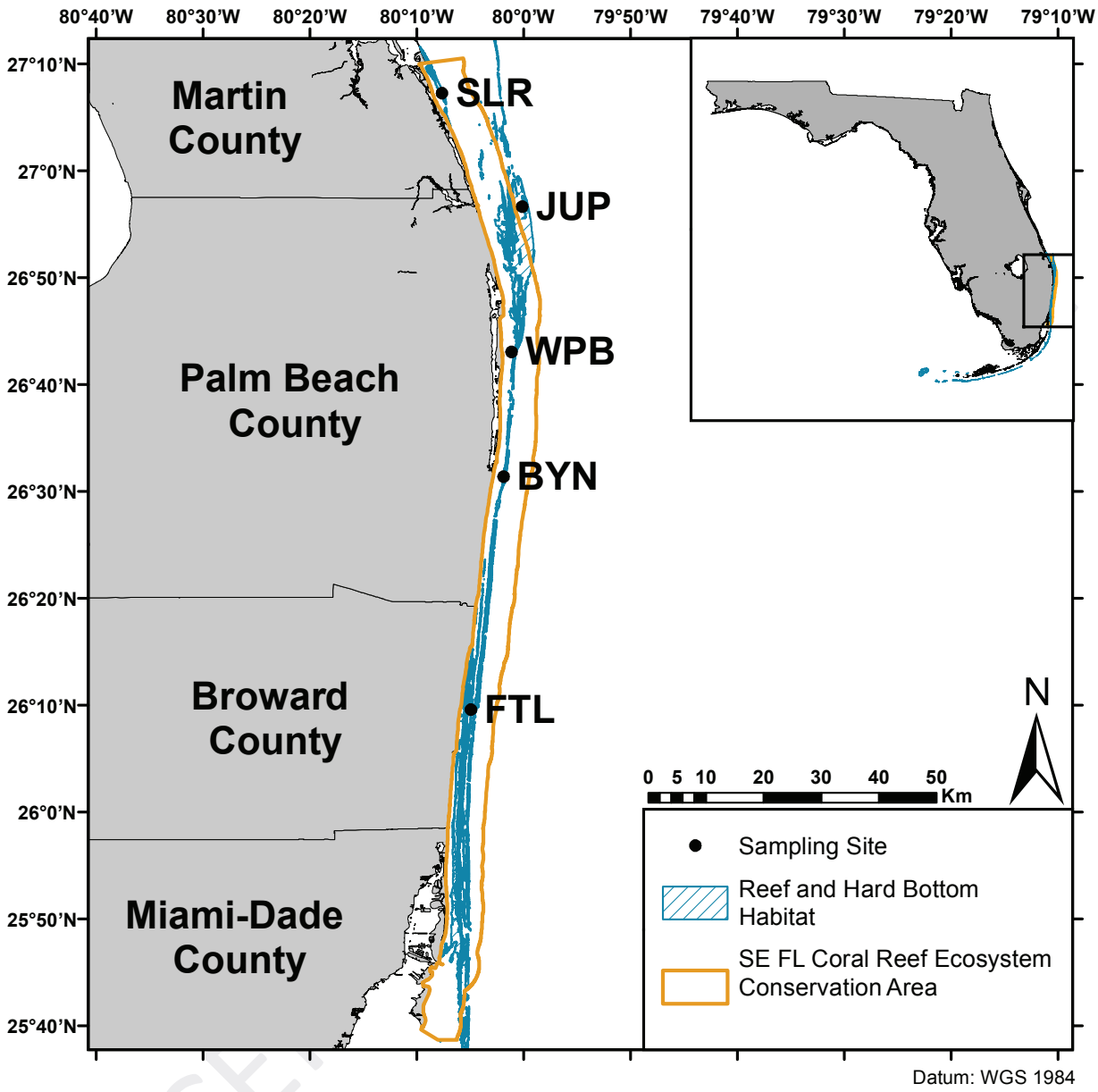


390

391 Figure 1. *Montastraea cavernosa* sampling locations on the northern Florida Reef Tract.
392 Populations were sampled at St. Lucie Reef (SLR), Jupiter (JUP), West Palm Beach (WPB),
393 Boynton Beach (BYN), and Fort Lauderdale (FTL). Overlays correspond to reef habitat
394 (shapefile source: Florida Fish and Wildlife Conservation Commission–Fish and Wildlife
395 Research Institute) and the Southeast Florida Coral Reef Ecosystem Conservation Area.

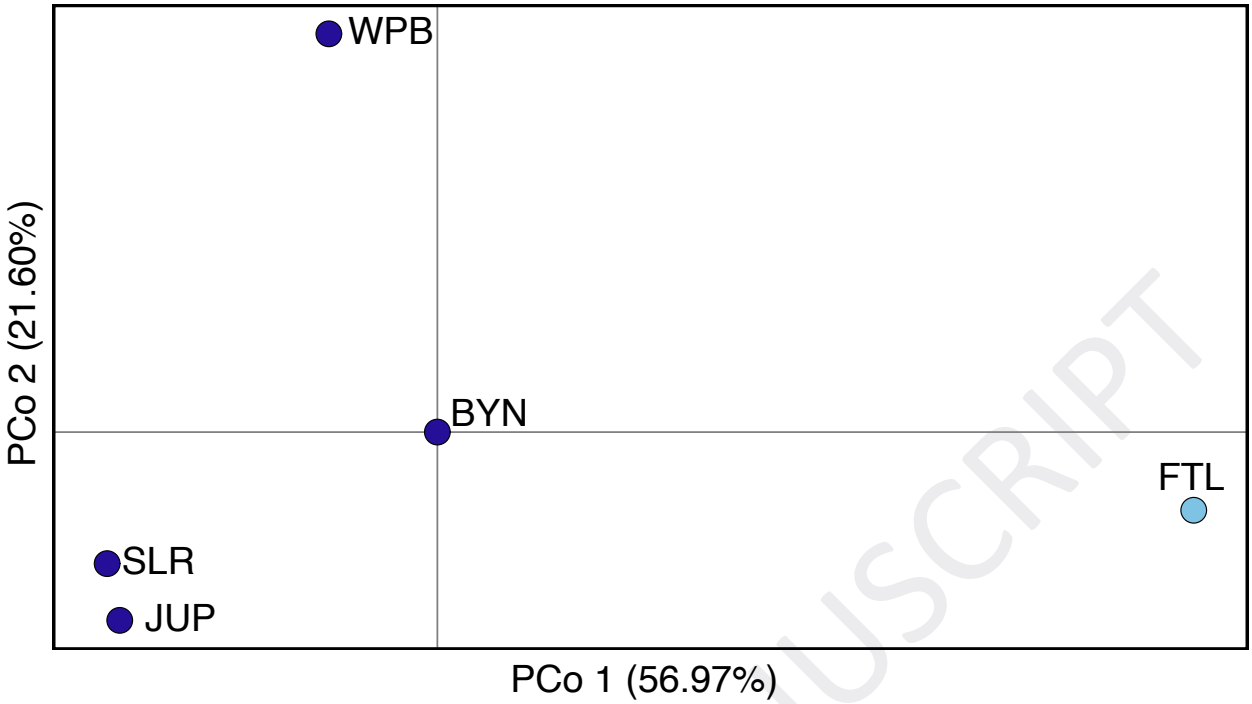


Figure 2. Principal coordinates analysis (PCoA) of Nei's genetic distance ($D_A$) among pairwise comparisons of populations, explaining 78.57% of the total genetic variation (PCo 1: 56.97%; PCo 2: 21.60%). Color of points correspond to the dominant genetic cluster identified in Structure analysis ($K$ = 2; Fig. 5).

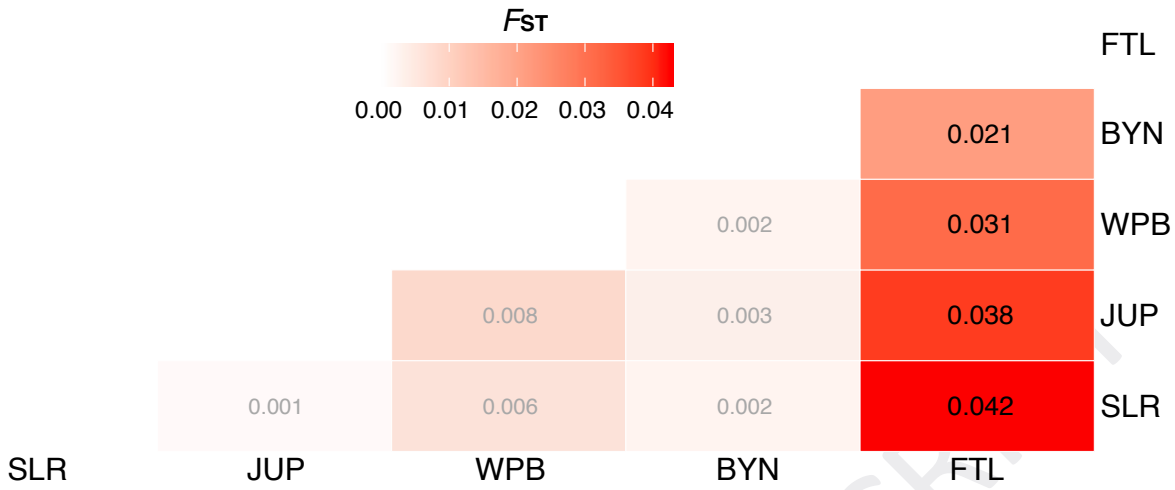


Figure 3. Pairwise $F_{ST}$ values among sampled geographic populations. Bolded values indicate significantly differentiated populations and color intensity reflects level of genetic differentiation from $F_{ST}$ values. Alpha was set at 0.05.

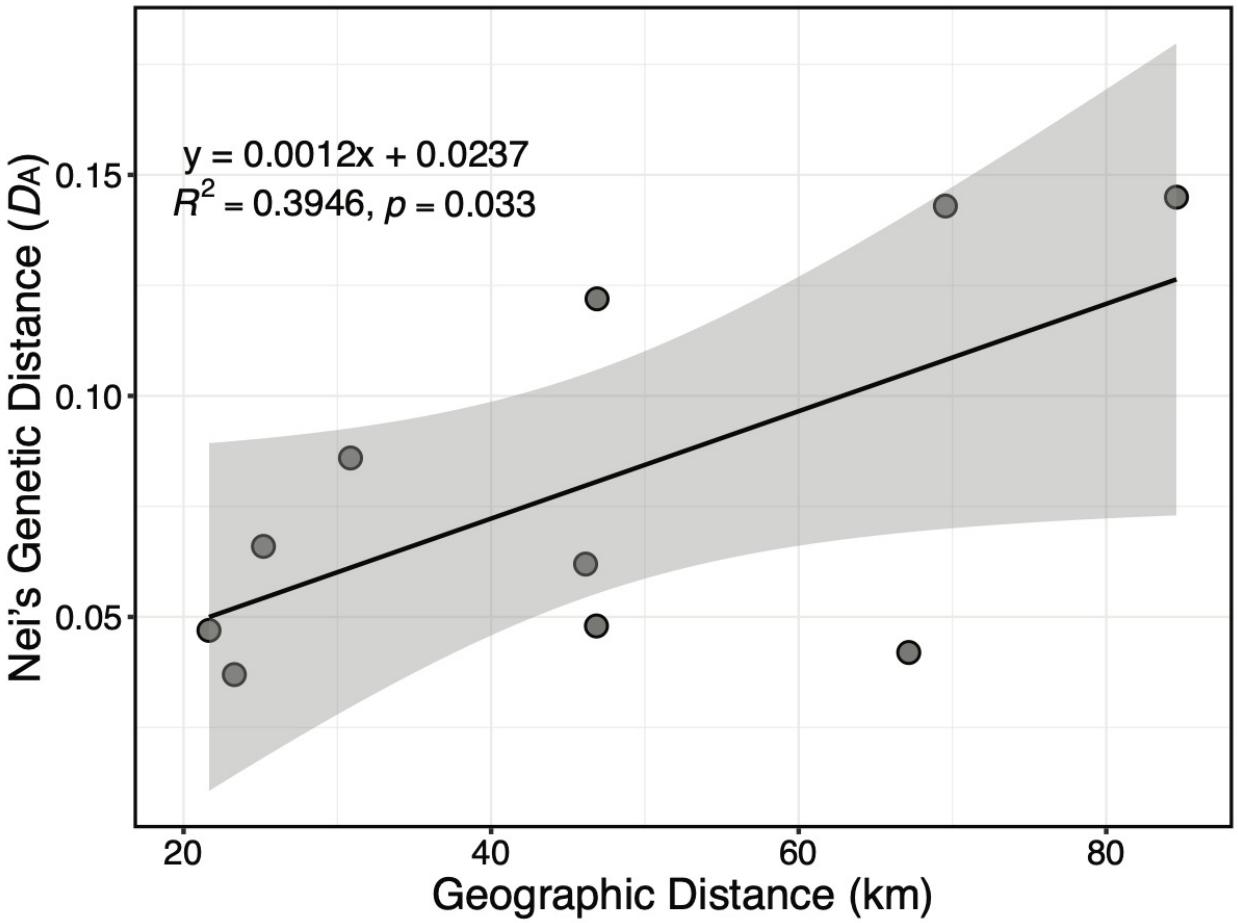


405

406 Figure 4. Mantel isolation by distance test relating Nei's genetic distance ($D_A$) to geographic
407 distance among pairwise comparisons of populations. Geographic isolation explained 39.46% of
408 observed genotypic variation among populations (Mantel test; $p < 0.033$, 999 permutations).

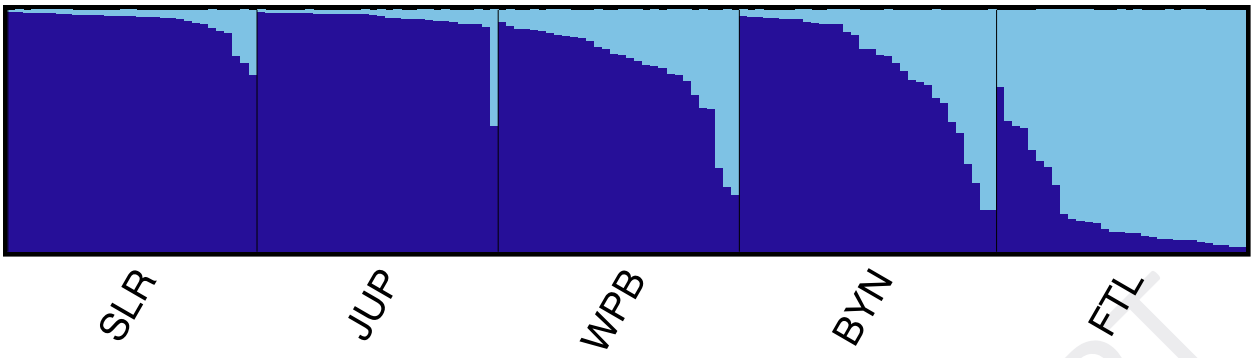


Figure 5. Genetic structure of *Montastraea cavernosa* populations in the northern Florida Reef Tract as predicted by Bayesian inference in Structure. Each column represents an individual *M. cavernosa* colony from the five geographic populations (x-axis). The relative height of each color (dark blue, light blue) represents the probability of membership to the genetic clusters ($K$ = 2).

415 **References**


416 Acosta A, Zea S. 1997. Sexual reproduction of the reef coral *Montastrea cavernosa*
417 (Scleractinia: Faviidae) in the Santa Marta area, Caribbean coast of Colombia. Marine
418 Biology 128: 141–148.
419 Aswani S, Mumby P, Baker AC, Christie P, McCook LJ, Steneck RS, Richmond RH. 2015.
420 Scientific frontiers in the management of coral reefs. Frontiers in Marine Science 2: 1–13.
421 Banks KW, Riegl BM, Richards VP, Walker BK, Helmle KP, Jordan LKB, Phipps J, Shivji MS,
422 Spieler RE, Dodge RE. 2008. The reef tract of continental Southeast Florida (Miami-Dade,
423 Broward and Palm Beach Counties, USA). Coral Reefs of the USA Dordrecht: Springer
424 Netherlands. p. 175–220.
425 Banks KW, Riegl BM, Shinn EA, Piller WE, Dodge RE. 2007. Geomorphology of the Southeast
426 Florida continental reef tract (Miami-Dade, Broward, and Palm Beach Counties, USA).
427 Coral Reefs 26: 617–633.
428 Baums IB, Johnson ME, Devlin-Durante MK, Miller MW. 2010. Host population genetic
429 structure and zooxanthellae diversity of two reef-building coral species along the Florida
430 Reef Tract and wider Caribbean. Coral Reefs 29: 835–842.
431 Beal J, Voss JD, Edge S, Cohen L. 2012. Assessment of coral stressors on St. Lucie Reef:
432 Florida's northernmost coral reef. Final Report for State Wildlife Grant. USFWS T-91-1,
433 Fort Pierce, FL. pp. 54.
434 Beerli P. 2006. Comparison of Bayesian and maximum-likelihood inference of population
435 genetic parameters. Bioinformatics 22: 341–345.
436 Beerli P, Palczewski M. 2010. Unified framework to evaluate panmixia and migration direction
437 among multiple sampling locations. Genetics 185: 313–326.
438 Beger M, Selkoe KA, Treml E, Barber PH, Von Der Heyden S, Crandall ED, Toonen RJ,
439 Riginos C. 2014. Evolving coral reef conservation with genetic information. Bulletin of
440 Marine Science 90: 159–185.
441 Benjamini Y, Hochberg Y. 1995. Controlling the false discovery rate: a practical and powerful
442 approach to multiple testing. Journal of the Royal Statistical Society: Series B
443 (Methodological) 57: 289–300.
444 Blacket MJ, Robin C, Good RT, Lee SF, Miller AD. 2012. Universal primers for fluorescent
445 labelling of PCR fragments-an efficient and cost-effective approach to genotyping by
446 fluorescence. Molecular Ecology Resources 12: 456–463.
447 Bongaerts P, Riginos C, Brunner R, Englebert N, Smith SR, Hoegh-Guldberg O. 2017. Deep
448 reefs are not universal refuges: reseeding potential varies among coral species. Science
449 Advances 3: e1602373.
450 Brazeau DA, Lesser MP, Slattery M. 2013. Genetic structure in the coral, *Montastraea*
451 *cavernosa*: assessing genetic differentiation among and within mesophotic reefs. PLoS
452 ONE 8: e65845.
453 Bruno JF, Selig ER. 2007. Regional decline of coral cover in the Indo-Pacific: Timing, extent,
454 and subregional comparisons. PLoS ONE 2: e711.
455 Burman SG, Aronson RB, van Woesik R. 2012. Biotic homogenization of coral assemblages
456 along the Florida reef tract. Marine Ecology Progress Series 467: 89–96.
457 Chapuis M-P, Estoup A. 2007. Microsatellite null alleles and estimation of population
458 differentiation. Molecular Biology and Evolution 24: 621–631.
459 Chomczynski P, Sacchi N. 2006. The single-step method of RNA isolation by acid guanidinium
460 thiocyanate–phenol–chloroform extraction: twenty-something years on. Nature Protocols 1:

581–585.
Collier C, Ruzicka R, Banks K, Barbieri L, Beal J, Bingham D, Bohnsack JA, Brooke S, Craig N, Dodge RE, Fisher LE, Gadbois N, Gilliam DS, Gregg L, Kellison T, Kosmynin VN, Lapointe B, McDevitt E, Phipps J, Poulos N, Proni J, Quinn P, Riegl B, Spieler RE, Walczak J, Walker BK, Warrick D. 2008. The state of coral reef ecosystems of Southeast Florida. In: J Waddel and A Clarke, editor. The state of coral reef ecosystems of the United States and Pacific Freely Associated States: 2008 NOAA Technical Memorandum NOS NCCOS 73. NOAA/NCCOS Center for Coastal Monitoring and Assessment's Biogeography Team. Silver Spring, MD: p. 131–160.
Cowen RK, Sponaugle S. 2009. Larval dispersal and marine population connectivity. Annual Review of Marine Science 1: 443–466.
Davies SW, Strader ME, Kool JT, Kenkel CD, Matz MV. 2017. Modeled differences of coral life-history traits influence the refugium potential of a remote Caribbean reef. Coral Reefs 36: 913–925.
Devlin-Durante MK, Miller MW, Precht WF, Baums IB, Carne L, Smith TB, Banaszak AT, Greer L, Irwin A, Fogarty ND, Williams DE. 2016. How old are you? Genet age estimates in a clonal animal. Molecular Ecology 25: 5628–5646.
Drury C, Schopmeyer S, Goergen E, Bartels E, Nedimyer K, Johnson M, Maxwell K, Galvan V, Manfrino C, Lirman D. 2017. Genomic patterns in *Acropora cervicornis* show extensive population structure and variable genetic diversity. Ecology and Evolution 7: 6188–6200.
Earl DA, VonHoldt BM. 2012. STRUCTURE HARVESTER: a website and program for visualizing STRUCTURE output and implementing the Evanno method. Conservation Genetics Resources 4: 359–361.
Eckert RJ, Studivan MS, Voss JD. 2019. Populations of the coral species *Montastraea cavernosa* on the Belize Barrier Reef lack vertical connectivity. Scientific Reports 9: 7200.
Edmunds PJ. 2015. A quarter-century demographic analysis of the Caribbean coral, *Orbicella annularis*, and projections of population size over the next century. Limnology and Oceanography 60: 840–855.
Evanno G, Regnaut S, Goudet J. 2005. Detecting the number of clusters of individuals using the software STRUCTURE: a simulation study. Molecular Ecology 14: 2611–2620.
Excoffier L, Lischer HEL. 2010. Arlequin suite ver 3.5: a new series of programs to perform population genetics analyses under Linux and Windows. Molecular Ecology Resources 10: 564–567.
Galindo HM, Olson DB, Palumbi SR. 2006. Seascape genetics: a coupled oceanographic-genetic model predicts population structure of Caribbean corals. Current Biology 16: 1622–1626.
Garavelli L, Studivan MS, Voss JD, Kuba A, Figueiredo J, Chérubin LM. 2018. Assessment of mesophotic coral ecosystem connectivity for proposed expansion of a marine sanctuary in the northwest Gulf of Mexico: larval dynamics. Frontiers in Marine Science 5: 174.
Gardner TA, Côté IM, Gill JA, Grant A, Watkinson AR. 2003. Long-term region-wide declines in Caribbean corals. Science 301: 958–960.
Gilliam DS, Walton CJ, Brinkhuis V, Ruzicka R, Colella M. 2015. Southeast Florida Coral Reef Evaluation and Monitoring Project 2014 Year 12 Final Report, Miami Beach, FL. pp. 43.
Goodbody-Gringley G, Woollacott RM, Giribet G. 2012. Population structure and connectivity in the Atlantic scleractinian coral *Montastraea cavernosa* (Linnaeus, 1767). Marine Ecology 33: 32–48.
Gutiérrez-Rodríguez C, Lasker HR. 2004. Microsatellite variation reveals high levels of genetic

variability and population structure in the gorgonian coral Pseudopterogorgia elisabethae across the Bahamas. Molecular ecology 13: 2211–2221.

Hare JA, Walsh HJ. 2007. Planktonic linkages among marine protected areas on the south Florida and southeast United States continental shelves. Canadian Journal of Fisheries and Aquatic Sciences 64: 1234–1247.

Hemond EM, Vollmer S V. 2010. Genetic diversity and connectivity in the threatened staghorn coral (Acropora cervicornis) in Florida. PLoS ONE 5: e8652.

Hughes TP. 1994. Catastrophes, phase shifts, and large-scale degradation of a Caribbean coral reef. Science 265: 1547–1551.

Jakobsson M, Rosenberg NA. 2007. CLUMPP: a cluster matching and permutation program for dealing with label switching and multimodality in analysis of population structure. Bioinformatics 23: 1801–1806.

Johns GM, Milon J, Sayers D. 2004. Socioeconomic study of reefs in Martin County, Florida. Report prepared for Martin County, Florida by Hazen and Sawyer, PC, Hollywood, FL. pp. 120.

Jones GP, Almany GR, Russ GR, Sale PF, Steneck RS, van Oppen MJH, Willis BL. 2009. Larval retention and connectivity among populations of corals and reef fishes: history, advances and challenges. Coral Reefs 28: 307–325.

Keenan K, McGinnity P, Cross TF, Crozier WW, Prodöhl PA. 2013. diveRsity: an R package for the estimation of population genetics parameters and their associated errors. Methods in Ecology and Evolution 4: 782–788.

Klepac CN, Beal J, Kenkel CD, Sproles A, Polinski JM, Williams MA, Matz MV, Voss JD. 2015. Seasonal stability of coral-*Symbiodinium* associations in the subtropical coral habitat of St. Lucie Reef, Florida. Marine Ecology Progress Series 532: 137–151.

Limouzy-Paris CB, Graber HC, Jones DL, Röpke AW, Richards WJ. 1997. Translocation of larval coral reef fishes via sub-mesoscale spin-off eddies from the Florida current. Bulletin of Marine Science 60: 966–983.

Lirman D, Fong P. 2007. Is proximity to land-based sources of coral stressors an appropriate measure of risk to coral reefs? An example from the Florida Reef Tract. Marine Pollution Bulletin 54: 779–791.

Lirman D, Schopmeyer S, Manzello D, Gramer LJ, Precht WF, Muller-Karger F, Banks K, Barnes B, Bartels E, Bourque A. 2011. Severe 2010 cold-water event caused unprecedented mortality to corals of the Florida Reef Tract and reversed previous survivorship patterns. PLoS ONE 6: e23047.

Lugo AE, Brown SB, Dodson R, Smith TS, Shugart HH. 1999. The Holdridge life zones of the conterminous United States in relation to ecosystem mapping. Journal of Biogeography 26: 1025–1038.

Manzello DP. 2015. Rapid recent warming of coral reefs in the Florida Keys. Scientific Reports 5: 16762.

Manzello DP, Matz MV, Enochs IC, Valentino L, Carlton RD, Kolodziej G, Serrano X, Towle EK, Jankulak M. 2019. Role of host genetics and heat-tolerant algal symbionts in sustaining populations of the endangered coral *Orbicella faveolata* in the Florida Keys with ocean warming. Global Change Biology 25: 1016–1031.

Mieog JC, van Oppen MJH, Berkelmans R, Stam WT, Olsen JL. 2009. Quantification of algal endosymbionts (*Symbiodinium*) in coral tissue using real-time PCR. Molecular Ecology Resources 9: 74–82.

553 Miller KJ, Howard CG. 2004. Isolation of microsatellites from two species of scleractinian coral.
554 Molecular Ecology Notes 4: 11–13.
555 Miller MW, Weil E, Szmant AM. 2000. Coral recruitment and juvenile mortality as structuring
556 factors for reef benthic communities in Biscayne National Park, USA. Coral Reefs 19: 115–
557 123.
558 Mumby PJ. 2009. Phase shifts and the stability of macroalgal communities on Caribbean coral
559 reefs. Coral Reefs 28: 761–773.
560 Mumby PJ, Hastings A, Edwards HJ. 2007. Thresholds and the resilience of Caribbean coral
561 reefs. Nature 450: 98–101.
562 Nunes FLD, Norris RD, Knowlton N. 2009. Implications of isolation and low genetic diversity in
563 peripheral populations of an amphi-Atlantic coral. Molecular Ecology 18: 4283–4297.
564 Nunes FLD, Norris RD, Knowlton N. 2011. Long distance dispersal and connectivity in amphi-
565 Atlantic corals at regional and basin scales. PLoS ONE 6: e22298.
566 Oey L, Ezer T, Lee H. 2005. Loop Current, rings and related circulation in the Gulf of Mexico: a
567 review of numerical models and future challenges. In: W Sturges and A Lugo-Fernandez,
568 editor. Circulation in the Gulf of Mexico: observations and models Washington DC:
569 American Geophysical Union. p. 31–56.
570 van Oppen MJH, Gates RD. 2006. Conservation genetics and the resilience of reef-building
571 corals. Molecular Ecology 15: 3863–3883.
572 Palandro DA, Hu C, Hallock P, Müller-Karger FE, Dustan P, Callahan MK, Kranenburg C,
573 Beaver CR. 2008. Quantification of two decades of shallow-water coral reef habitat decline
574 in the Florida Keys National Marine Sanctuary using Landsat data (1984–2002). Remote
575 Sensing of Environment 112: 3388–3399.
576 Palumbi SR. 2003. Population genetics, demographic connectivity, and the design of marine
577 reserves. Ecological Applications 13: 146–158.
578 Palumbi SR. 2004. Marine reserves and ocean neighborhoods: the spatial scale of marine
579 populations and their management. Annual Review of Environment and Resources 31–68.
580 Peakall R, Smouse PE. 2012. GenAlEx 6.5: genetic analysis in Excel. Population genetic
581 software for teaching and research–an update. Bioinformatics 28: 2537–2539.
582 Porto-Hannes I, Zubillaga AL, Shearer TL, Bastidas C, Salazar C, Coffroth MA, Szmant AM.
583 2015. Population structure of the corals *Orbicella faveolata* and *Acropora palmata* in the
584 Mesoamerican Barrier Reef System with comparisons over Caribbean basin-wide spatial
585 scale. Marine Biology 162: 81–98.
586 Precht WF, Gintert BE, Robbart ML, Fura R, van Woesik R. 2016. Unprecedented Disease-
587 Related Coral Mortality in Southeastern Florida. Scientific Reports 6: 31374.
588 Pritchard JK, Stephens M, Donnelly P. 2000. Inference of population structure using multilocus
589 genotype data. Genetics 155: 945–959.
590 Reed JK. 1985. Deepest distribution of Atlantic hermatypic corals discovered in the Bahamas.
591 Proceedings of the 5th International Coral Reef Congress, Tahiti 6: 249–254.
592 Rosenberg NA. 2004. DISTRUCT: a program for the graphical display of population structure.
593 Molecular Ecology Notes 4: 137–138.
594 Ruzicka RR, Colella MA, Porter JW, Morrison JM, Kidney JA, Brinkhuis V, Lunz KS,
595 MacAulay KA, Bartlett LA, Meyers MK, Colee J. 2013. Temporal changes in benthic
596 assemblages on Florida Keys reefs 11 years after the 1997/1998 El Niño. Marine Ecology
597 Progress Series 489: 125–141.
598 Schuelke M. 2000. An economic method for the fluorescent labeling of PCR fragments. Nature

Biotechnology 18: 233–234.
Serrano XM, Baums IB, O'Reilly K, Smith TB, Jones RJ, Shearer TL, Nunes FLD, Baker AC. 2014. Geographic differences in vertical connectivity in the Caribbean coral *Montastraea cavernosa* despite high levels of horizontal connectivity at shallow depths. Molecular Ecology 23: 4226–4240.
Serrano XM, Baums IB, Smith TB, Jones RJ, Shearer TL, Baker AC. 2016. Long-distance dispersal and vertical gene flow in the Caribbean brooding coral *Porites astreoides*. Scientific Reports 6: 21619.
Shearer TL, Coffroth MA. 2004. Isolation of microsatellite loci from the scleractinian corals, *Montastraea cavernosa* and *Porites astreoides*. Molecular Ecology Notes 4: 435–437.
Soong K. 1993. Colony size as a species character in massive reef corals. Coral Reefs 12: 77–83.
Sponaugle S, Cowen RK. 2019. Coral Ecosystem Connectivity Between Pulley Ridge and the Florida Keys. In: Y Loya, KA Puglise, and TCL Bridge, editor. Mesophotic Coral Ecosystems, Coral Reefs of the World 12 Springer Nature Switzerland. p. 897–907.
Sponaugle S, Lee T, Kourafalou V, Pinkard D. 2005. Florida Current frontal eddies and the settlement of coral reef fishes. Limnology and Oceanography 50: 1033–1048.
Studivan MS, Voss JD. 2018a. Population connectivity among shallow and mesophotic *Montastraea cavernosa* corals in the Gulf of Mexico identifies potential for refugia. Coral Reefs 37: 1183–1196.
Studivan MS, Voss JD. 2018b. Assessment of mesophotic coral ecosystem connectivity for proposed expansion of a marine sanctuary in the Northwest Gulf of Mexico: population genetics. Frontiers in Marine Science 5: 152.
Szmant AM. 1991. Sexual reproduction by the Caribbean reef corals *Montastrea annularis* and *M. cavernosa*. Marine Ecology Progress Series 74: 13–25.
Vermeij MJA, Fogarty ND, Miller MW. 2006. Pelagic conditions affect larval behavior, survival, and settlement patterns in the Caribbean coral *Montastraea faveolata*. Marine Ecology Progress Series 310: 119–128.
Walker BK. 2012. Spatial analyses of benthic habitats to define coral reef ecosystem regions and potential biogeographic boundaries along a latitudinal gradient. PLoS ONE 7: e30466.
Walker BK, Gilliam DS. 2013. Determining the extent and characterizing coral reef habitats of the northern latitudes of the Florida Reef Tract (Martin County). PLoS ONE 8: e80439.
Walton CJ, Hayes NK, Gilliam DS. 2018. Impacts of a regional, multi-year, multi-species coral disease outbreak in Southeast Florida. Frontiers in Marine Science 5: 323.
Ward TJ, Heinemann D, Evans N. 2001. The role of marine reserves as fisheries management tools. A review of concepts, evidence and international experience. Bureau of Rural Sciences, Canberra, Australia. pp. 192.

636 **Supplementary Materials**

637 Table S1: Primer and fluorescently-labeled universal tail sequences for *Montastraea cavernosa* microsatellite loci amplified in three
638 triplex reactions. Loci as in Serrano *et al.* (2014); universal tails as in Schuelke (2000).

| Plex | Locus | Primer Name | Primer Sequence (5' - 3') | Universal Tail | Tail Sequence (5' - 3') |
|---|---|---|---|---|---|
| 1 | MC29 | MC29_F | CAGGACCAGGCTACCGTGCTCCTTGGTCACCCTACAA | C | NED-CAGGACCAGGCTACCGTG |
| | | MC29_R | GGTGAAGAAGCAGCCATTGG | | |
| | MC41 | MC41_F | GCCTCCCTCGCGCCAAATTACGCAACACTGTGCA | A | 6FAM-GCCTCCCTCGCGCCA |
| | | MC41_R | TCGACTGACCGAAGTACCT | | |
| | MC49 | MC49_F | GCCTTGCCAGCCCGCATTCCTCCAGTGATGTACCT | B | VIC-GCCTTGCCAGCCCGC |
| | | MC49_R | CTGAGTTCCTGCCATTAGG | | |
| 2 | MC46 | MC46_F | CAGGACCAGGCTACCGTGCGGTGTAGCTCTAGCAGGA | C | NED-CAGGACCAGGCTACCGTG |
| | | MC46_R | ACTGAGTCGCAGCATTTGG | | |
| | MC65 | MC65_F | GCCTCCCTCGCGCCATTTGTGATTGGCCAGGGTG | A | 6FAM-GCCTCCCTCGCGCCA |
| | | MC65_R | TTGTGCTGTGAAGCATGAT | | |
| | MC97 | MC97_F | GCCTTGCCAGCCCGCACATGTGGCCTTGTTACCA | B | VIC-GCCTTGCCAGCCCGC |
| | | MC97_R | CGAACATCAGTGACAACCT | | |
| 3 | MC4 | MC4_F | CAGGACCAGGCTACCGTGACGATCAAGACTCCAACGA | C | NED-CAGGACCAGGCTACCGTG |
| | | MC4_R | GCTCTTCGTGAACACTGAGG | | |
| | MC18 | MC18_F | GCCTCCCTCGCGCCAGGAGAACTGGATACCATGTC | A | 6FAM-GCCTCCCTCGCGCCA |

| | | | | |
|---|---|---|---|---|
| | MC18_R | TATGGTCCTGGGACAACTT | | |
| MC114 | MC114_F | GCCTTGCCAGCCCGCACTGTAGATCGAGGCGTTTC | B | VIC-GCCTTGCCAGCCCGC |
| | MC114_R | TCTGTTCCTCTGACTCTTTCG | | |

639

Table S2. Genetic diversity statistics across populations and loci. $N_g$: number of samples, $N_a$: number of alleles, $N_{pa}$: number of private alleles, $A_r$: allelic richness, $H_o$: observed heterozygosity, $H_e$: expected heterozygosity, $P_{HWE}$: FDR-corrected $p$-values for tests of Hardy Weinberg Equilibrium. Insignificant ($p$>0.05) HWE test results denoted as ns. Statistics presented for locus MC4, which were evaluated prior to the removal of the locus from subsequent analyses.

| Population | Statistic | MC29 | MC41 | MC49 | MC46 | MC65 | MC97 | MC4 | MC18 | MC114 |
|---|---|---|---|---|---|---|---|---|---|---|
| SLR | $N_g$ | 31 | 27 | 26 | 30 | 31 | 30 | 23 | 28 | 27 |
| | $N_a$ | 8 | 6 | 5 | 4 | 6 | 6 | 20 | 10 | 16 |
| | $N_{pa}$ | 1 | 0 | 0 | 0 | 0 | 0 | 1 | 0 | 1 |
| | $A_r$ | 7.18 | 5.60 | 4.55 | 3.45 | 5.17 | 5.59 | 15.40 | 9.08 | 14.05 |
| | $H_o$ | 0.839 | 0.630 | 0.423 | 0.500 | 0.452 | 0.667 | 0.696 | 0.679 | 0.963 |
| | $H_e$ | 0.779 | 0.773 | 0.533 | 0.446 | 0.491 | 0.614 | 0.922 | 0.869 | 0.909 |
| | $P_{HWE}$ | ns | 0.008 | ns | ns | ns | ns | 0.028 | ns | ns |
| JUP | $N_g$ | 28 | 30 | 27 | 30 | 30 | 30 | 30 | 30 | 30 |
| | $N_a$ | 7 | 6 | 11 | 4 | 5 | 7 | 30 | 9 | 13 |
| | $N_{pa}$ | 0 | 0 | 4 | 0 | 0 | 0 | 5 | 0 | 1 |
| | $A_r$ | 6.58 | 5.94 | 8.95 | 3.75 | 4.65 | 6.62 | 22.75 | 8.34 | 12.27 |
| | $H_o$ | 0.821 | 0.633 | 0.630 | 0.533 | 0.667 | 0.733 | 0.767 | 0.833 | 0.967 |
| | $H_e$ | 0.767 | 0.724 | 0.698 | 0.453 | 0.574 | 0.728 | 0.951 | 0.828 | 0.898 |
| | $P_{HWE}$ | ns | ns | ns | ns | ns | ns | ns | ns | ns |
| WPB | $N_g$ | 30 | 27 | 28 | 27 | 27 | 29 | 27 | 29 | 29 |
| | $N_a$ | 6 | 7 | 7 | 4 | 5 | 6 | 27 | 11 | 15 |
| | $N_{pa}$ | 0 | 1 | 0 | 0 | 0 | 0 | 4 | 0 | 1 |
| | $A_r$ | 5.95 | 6.16 | 6.50 | 3.28 | 4.43 | 5.48 | 20.30 | 9.28 | 13.38 |
| | $H_o$ | 0.733 | 0.630 | 0.643 | 0.778 | 0.333 | 0.621 | 0.741 | 0.586 | 0.690 |
| | $H_e$ | 0.784 | 0.733 | 0.732 | 0.502 | 0.405 | 0.642 | 0.941 | 0.798 | 0.910 |
| | $P_{HWE}$ | ns | ns | 0.008 | ns | ns | ns | 0.008 | ns | ns |

| | | | | | | | | | | |
|---|---|---|---|---|---|---|---|---|---|---|
| BYN | $N_g$ | 32 | 32 | 32 | 31 | 31 | 31 | 31 | 31 | 32 |
| | $N_a$ | 8 | 8 | 8 | 5 | 5 | 6 | 25 | 11 | 12 |
| | $N_{pa}$ | 0 | 0 | 1 | 0 | 0 | 1 | 3 | 0 | 0 |
| | $A_r$ | 6.98 | 7.11 | 6.85 | 4.43 | 4.71 | 5.69 | 19.62 | 10.59 | 11.44 |
| | $H_o$ | 0.625 | 0.813 | 0.688 | 0.452 | 0.452 | 0.645 | 0.806 | 0.871 | 0.813 |
| | $H_e$ | 0.775 | 0.768 | 0.655 | 0.401 | 0.404 | 0.688 | 0.942 | 0.850 | 0.899 |
| | $P_{HWE}$ | ns | ns | ns | ns | ns | ns | ns | ns | ns |
| FTL | $N_g$ | 30 | 28 | 29 | 30 | 29 | 30 | 29 | 31 | 31 |
| | $N_a$ | 8 | 6 | 13 | 3 | 4 | 5 | 24 | 10 | 12 |
| | $N_{pa}$ | 0 | 0 | 4 | 0 | 0 | 0 | 4 | 1 | 0 |
| | $A_r$ | 7.28 | 5.58 | 11.41 | 2.79 | 3.84 | 4.96 | 19.45 | 8.73 | 10.50 |
| | $H_o$ | 0.633 | 0.643 | 0.655 | 0.167 | 0.379 | 0.700 | 0.690 | 0.742 | 0.806 |
| | $H_e$ | 0.767 | 0.672 | 0.881 | 0.156 | 0.330 | 0.707 | 0.937 | 0.848 | 0.857 |
| | $P_{HWE}$ | ns | ns | 0.028 | ns | ns | ns | 0.008 | ns | ns |

646

647 Table S3. Cluster selection methods for population structure analysis. Comparison of model log
648 likelihoods (Mean LnP(*K*)) and stepwise change in model likelihood (Δ*K*) used for the Evanno
649 method to determine the most likely number of genetic clusters (*K*), indicated in bold.

| **K** | **Mean LnP(*K*)** | **Stdev LnP(*K*)** | **Ln'(*K*)** | **\|Ln''(*K*)\|** | **Δ*K*** |
|---|---|---|---|---|---|
| 1 | -3962 | 0.25 | | | |
| **2** | **-3922** | **10.77** | **39.71** | **258.37** | **23.99** |
| 3 | -4141 | 89.74 | -218.66 | 116.60 | 1.30 |
| 4 | -4476 | 160.98 | -335.26 | 95.73 | 0.59 |
| 5 | -4716 | 288.89 | -239.53 | 25.57 | 0.09 |
| 6 | -4930 | 450.94 | -213.96 | 282.95 | 0.63 |
| 7 | -5427 | 489.48 | -496.91 | 729.37 | 1.49 |
| 8 | -5194 | 390.34 | 232.46 | | |

650

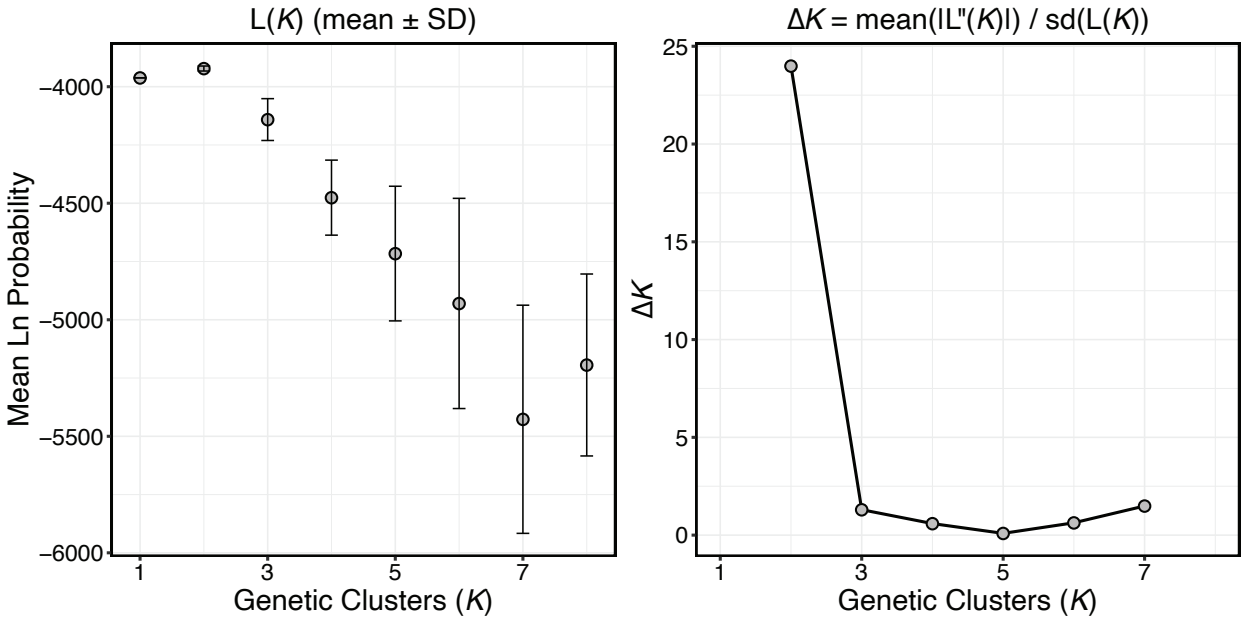


Figure S1. Cluster selection methods for population structure analysis. Comparison of model log likelihoods (left) and stepwise change in model likelihood ($\Delta K$; right) used for the Evanno method to determine the most likely number of genetic clusters ($K$). Error bars represent standard deviation.